Paper No. 11-2687

Development of a Low-Cost, Energy-Absorbing, Bridge Rail

by

Jeffrey C. Thiele, M.S.C.E, E.I.T.
DLR Group
1111 Lincoln Mall
Lincoln, Nebraska 68508
Phone: (402) 742-4200
Email: jthiele@dlrgroup.com

Dean L. Sicking, Ph.D., P.E.
Midwest Roadside Safety Facility
University of Nebraska-Lincoln
130 Whittier Building
2200 Vine Street
Lincoln, Nebraska 68583-0853
Phone: (402) 472-9332
Fax: (402) 472-2022
Email: dsicking@unl.edu

Ronald K. Faller, Ph.D., P.E.
Midwest Roadside Safety Facility
University of Nebraska-Lincoln
130 Whittier Building
2200 Vine Street
Lincoln, Nebraska 68583-0853
Phone: (402) 472-6864
Fax: (402) 472-2022
Email: rfaller1@unl.edu

Karla A. Lechtenberg, M.S.M.E., E.I.T.
Midwest Roadside Safety Facility
University of Nebraska-Lincoln
130 Whittier Building
2200 Vine Street
Lincoln, Nebraska 68583-0853
Phone: (402) 472-9070
Fax: (402) 472-2022
Email: kpolivka2@unl.edu
(Corresponding Author)

Robert W. Bielenberg, M.S.M.E., E.I.T.
Midwest Roadside Safety Facility
University of Nebraska-Lincoln
130 Whittier Building
2200 Vine Street
Lincoln, Nebraska 68583-0853
Phone: (402) 472-9064
Fax: (402) 472-2022
Email: rbielenberg2@unl.edu

John D. Reid, Ph.D.
Mechanical Engineering Department
Midwest Roadside Safety Facility
University of Nebraska-Lincoln
N104 WSEC
Lincoln, Nebraska 68588-0656
Phone: (402) 472-3084
Fax: (402) 472-1467
Email: jreid@unl.edu

Scott K. Rosenbaugh, M.S.C.E., E.I.T.
Midwest Roadside Safety Facility
University of Nebraska-Lincoln
130 Whittier Building
2200 Vine Street
Lincoln, Nebraska 68583-0853
Phone: (402) 472-9324
Fax: (402) 472-2022
Email: srosenba@unlserve.unl.edu

Submitted to

Transportation Research Board
90th Annual Meeting
January 23-27, 2011
Washington, D.C.

March 15, 2011

Length of Paper: 6,819 (text) + 2,250 (5 figures and 4 tables) = 9,069 words

ABSTRACT

A new, low-cost bridge railing was designed to be compatible with the Midwest Guardrail System (MGS). The barrier system was configured in a manner that reduced bridge deck width and its associated cost.

Several concepts for an energy-absorbing bridge post were developed and tested, including strong-post designs with plastic hinges and weak-post designs with bending near the bridge deck attachment,. The final railing concept incorporated S3x5.7 (S76x8.5) steel posts housed in a tubular bracket placed at the outside vertical edge of the deck and anchored to the top and bottom of the deck with one through-deck bolt. The W-beam rail section was attached to the posts with a bolt that was designed to fracture during an impact event.

Two full-scale crash tests were performed according to the Test Level 3 impact conditions provided in the *Manual for Assessing Safety Hardware* (MASH). The bridge rail system successfully met all safety performance criteria for both the small car and pickup truck crash tests. BARRIER VII computer simulations, in combination with the full-scale crash testing programs for the bridge railing and MGS, demonstrated that a special approach guardrail transition was unnecessary.

Keywords: Bridge Rail, Approach Guardrail Transition, Energy-Absorbing, MGS, MASH, TL-3, Crash Testing

INTRODUCTION

Existing bridge rail systems are generally costly and much stiffer than approach guardrails. This difference in stiffness necessitates the inclusion of stiffness transitions between the two barrier systems, which are also costly to install. A bridge rail with comparable lateral stiffness, strength, and geometry to that of an approach guardrail system embedded in soil could eliminate the need for costly transition sections. Additionally, a more flexible bridge rail system that uses less material than existing bridge rails could substantially reduce overall construction costs for the bridge rail and deck and decrease the dead loads applied to the bridge. Previously-developed barrier systems, such as guardrails for attachment to low-fill culverts and long-span guardrails, provide such solutions for concrete box culverts. However, their viability has been limited to shorter span lengths. Thus, a new railing was desired for use with longer span bridges. The new railing system would be ideal for low-volume, high-speed, highway applications, in which the expected frequency of vehicle impacts is low and the need for controlling construction costs is high. The low initial cost and low frequency of crashes may outweigh repair costs, thus resulting in decreased life-cycle costs.

RESEARCH OBJECTIVE

The purpose of this research study was to develop a bridge rail design based on the Midwest Guardrail System (MGS) that would satisfy the Test Level 3 (TL-3) criteria described in the *Manual for Assessing Safety Hardware* (MASH) [1] and eliminate the need for an approach guardrail transition when used with the MGS [2-6]. The new bridge rail was to:

1. be suitable for use on bridges or culverts with spans greater than 25 ft (7.62 m);
2. provide comparable lateral stiffness and strength to the standard MGS;
3. allow controlled post rotation when lateral loads become high; and
4. provide a yielding post or post-to-deck connection that mitigates bridge deck damage during most vehicular impacts.

BARRIER DESIGN

Two important components of the new bridge rail were the post-to-deck and post-to-rail connections. To eliminate the need for an approach guardrail transition, the post design was required to develop rail stiffness, strength, and deflection characteristics comparable to those of guardrail posts embedded in soil. Further, a post system was needed that would transmit loads into the bridge deck without causing damage during most impacts. It was also desirable to minimize barrier encroachment onto the deck surface in order to reduce bridge construction costs. Finally, the post design and mounting system needed to be simple, economical, and usable on both newly constructed bridges as well as for retrofitting existing structures.

Post-to-Deck Connection

The new bridge rail post was required to provide sufficient stiffness and strength to match the lateral deflection of the MGS and also absorb sufficient energy to limit rail tensile loading. Two design approaches were pursued and included: (1) a strong-post system with a plastic hinge

designed to allow deflection at a prescribed load and (2) a weak-post system designed to bend the post at its base.

Two of the numerous strong-post concepts were further evaluated through dynamic component testing, as discussed in the research reports [7,8]. One concept utilized a steel plate welded to a post and anchored to the top of the deck with a through-deck bolt with the post placed on the outer vertical edge of the deck. During post rotation, the bolt tears through the plate, which generates a relatively constant resistive force. The through-deck bolt bends when loaded and applies out-of-plane stress to the plate to help initiate tearing. Placement of the post on the side of the deck minimized rail intrusion onto the deck; however, the plate extended onto the deck surface several inches past the rail and could potentially encounter damage from snow plows. Bolt preload and friction could potentially prevent plate movement and tearing. Thus, a rudimentary mechanism was designed into the system to limit preload and friction, but its effectiveness was unknown.

The second strong-post concept utilized gusseted anchor brackets that were side-mounted to the bridge deck with a tubular post placed in the bracket and connected with a horizontal bolt that tore through both side faces of the post upon post rotation. The angled, deck anchor brackets were configured to prevent bolt preload from clamping the post as well as ensure that friction would not adversely affect post resistance. However, the mounting brackets were expensive, since they required significant strength in order to be reusable.

While dynamic component testing of the strong-post concepts demonstrated the potential to develop the desired resistive forces for the bridge rail, the strong-post designs faced two major problems. First, it was difficult to obtain the desired behavior in the steel tear-out mechanism, thus requiring more elaborate and expensive systems than originally envisioned. Second, the load transmitted from the post into the deck was quite large and was believed to have the potential for damaging the bridge deck. Due to the flexible nature of the rail, the load would be localized to posts near the point of impact, rather than distributed to a larger number of posts as with a stiffer rail. To distribute the load through a larger portion of the deck, larger and more expensive post-to-deck connections would be required. Third, the strong-post design posed an increased potential for vehicle wheels to snag on strong posts. For these reasons, the strong-post system was abandoned in favor of a weak-post bridge rail.

The weak-post concepts utilized S3x5.7 (S76x8.5) steel posts based on their demonstrated performance and use in existing guardrail systems. Prior research has shown these posts generate roughly one-half the resistive force and energy absorption of standard W6x9 (W152x13.4) guardrail posts embedded in soil. Thus, S-posts placed with half-post spacing, or 37½ in. (953 mm) should provide similar lateral stiffness, strength, and deflection characteristics to that provided by the MGS.

A post-to-deck connection which allowed for the post to be essentially rigid at its base but be quickly replaced or repaired following an impact was deemed necessary. It was desired that the post-to-deck attachment hardware and the bridge deck should not be damaged during a vehicular crash. Two of the numerous concepts for the post-to-deck connections were further evaluated through dynamic component testing, as discussed in the referenced reports [7, 8]. One concept utilized a side-mounted, bent plate socket, while the other concept utilized a mounting tube anchored to the deck with a vertical, through-deck bolt.

Dynamic bogie testing was also used to evaluate the weak post concept post-to-deck connection systems. Although both weak-post concept tests were unsuccessful due to inadequate strength of the deck anchorage system, the weak-post systems imparted lower loading into the

deck and provided a decreased propensity for wheel snag on the posts as compared to the strong-post options. BARRIER VII computer simulation also showed that the weak-post system with a half-post spacing provided similar lateral stiffness and strength to that of the MGS. Thus, a weak-post design was selected, but special steel reinforcement was designed for use with the reinforced concrete bridge deck to ensure the structural adequacy requirements were met. Note that the bridge railing system can be retrofitted to existing bridge decks as long as the deck reinforcement can withstand the required loads.

Post-to-Rail Connection

The barrier's post-to-rail connection must have sufficient strength to prevent premature guardrail release from the posts downstream of the vehicle, which may result in vehicle override of the barrier. However, the connection must also be sufficiently weak such that it does not allow the rail to be pulled down by the rotating posts, another cause of vehicle override. Guardrail release is an important consideration in barrier systems which do not utilize blockouts. The offset blocks help maintain rail height during post rotation. Ideally, the post-to-rail connection would utilize standard and readily-available components. A variety of post-to-rail connections were developed and are shown in the research report [7,8]. However, the standard G2 weak-post guardrail connection was selected to form the basis for the final design.

The G2 connection utilized a $^{5}/_{16}$-in. (7.9-mm) diameter, ASTM A307 Grade A bolt, a hex nut, and a 1¾-in. (44-mm) ASTM A36 square washer. This low-cost connection was deemed sufficient to provide adequate ductility to absorb stress waves that pass through the W-beam rail with the deformation of the washer and slot. Although this G2 connection was believed to fail prematurely in a previous research study involving weak-post guardrail [9], the new bridge rail would be supported by more posts due to the use of a 37½ in. (953 mm) post spacing versus the 16 ft (4.9 m) G2 post spacing, thus making premature release far less likely. Shelf bolts, used in the standard G2 connection, were not deemed necessary for resisting environmental loads due to the shorter unsupported length.

Static testing was used to evaluate the performance of the G2 post-to-rail connection with two different bolt sizes. Bolt diameters of $^{5}/_{16}$ in. (7.9 mm) and ⅜ in. (9.5 in.) were tested under conditions which represented the extreme limits of system performance. Two tests investigated the maximum load capacity of the connection, which would occur when the bolt and washer were positioned at the end of the guardrail slot at a splice location (i.e. 2 layers of guardrail). For another test, the bolt was positioned at the center of the guardrail slot in a single layer of guardrail to determine a lower bound for expected connection failure force. For all tests, the bolt was pulled at an angle normal to the W-beam. Results of these tests are shown in Table 1.

Following the static testing, a $^{5}/_{16}$-in. (7.9-mm) diameter, ASTM A307 Grade A bolt was selected for use. Worst-case loading conditions resulted in a maximum failure load of 4.3 kips (18.7 kN), at which point the bolt fractured. This relatively low failure load would ensure that the rail would not be pulled downward during post rotation or result in vehicle override of the barrier.

Prior crash testing of weak-post, W-beam guardrail systems has demonstrated a propensity for rail rupture [10-13]. These rail ruptures were attributed to small cuts or nicks in the guardrail produced by the sharp edges of post flanges. Thus, it was decided to allow the placement of guardrail splices at post locations as long as 6-in. (152-mm) long, W-beam backup plates were placed at all post locations, as this pattern would not require special punching of guardrail sections.

BARRIER VII ANALYSIS

Introduction

BARRIER VII [14] simulations were performed to determine if the weak-post bridge rail with half-post spacing would generate comparable lateral stiffness, strength, and deflections to that observed for the MGS. The primary simulation results of interest were pocketing angles developed in the barrier near the front of the vehicle. Prior safety studies of barrier transitions have reported it desirable to limit the maximum guardrail pocketing angle to less than 30 degrees [15-16]. Simulated pocketing angles were measured using linear regression lines fit to both three and five consecutive nodes of the barrier. Five-node pocketing angles were preferred for the analysis, as the longer length of rail created a more representative pocketing condition, and using shorter lengths of rail may overestimate the severity of pocketing.

Wheel snag on vertical posts was not considered in the simulation analysis. The use of 12-in. (305-mm) deep blockouts with the MGS has demonstrated limited concern for wheel snag during previous crash tests [2-6]. The S3x5.7 (S76x8.5) weak posts have also been widely used in non-blocked barrier systems, including weak-post W-beam and cable guardrails. Crash testing of these weak-post barrier systems has shown that wheel snag on S3x5.7 (S76x8.5) steel posts does not pose a significant safety concern.

Model Input Description

Three S3x5.7 (S76x8.5) post models used in the simulations were created from previously-performed dynamic bogie tests [17] in which rigidly-mounted posts were impacted at angles of 90, 75, and 60 degrees with respect to their strong axes. Force vs. deflection curves were used to determine post behavior perpendicular to the longitudinal axis of the barrier (strong-axis bending). Post behavior parallel to the barrier (weak-axis bending) was determined using elastic bending equations.

Two models of W6x8.5 (W152x12.6) posts were developed for the simulations. A model of W6x8.5 (W152x12.6) posts was taken from previously-developed BARRIER VII simulations calibrated to full-scale crash tests of the MGS [2,18-19]. A second post model with increased resistive force was developed based on the soil strength requirements stipulated in Appendix B of MASH. Anchor post models were previously developed based on modified breakaway cable terminal (BCT) post assemblies used to replicate the tensile capacity of tangent guardrail installations [20]. The W-beam guardrail model was determined using the geometry and material properties of standard 12-gauge (2.66-mm thick) corrugated guardrail combined with the elastic bending equations. A previously-calibrated, coefficient of friction equal to 0.35 was used for the MGS [1, 18].

Two vehicle models, developed by MwRSF personnel under NCHRP Project No. 22-14(2), were used in the MASH simulations. Two mesh densities were used for the 175-ft (53.34-m) simulated barriers that utilized node spacings of 9⅜ in. (238 mm) and $4^{11}/_{16}$ in. (119 mm), resulting in 225 and 449 total nodes, respectively. Full input parameters for BARRIER VII models are available in the referenced report [7].

Simulation Results

A series of barrier models were developed for comparison of maximum barrier deflections and pocketing angles for the MGS and the proposed bridge rail design, as shown in Table 2. A barrier system consisting of standard MGS and simulated end anchor terminals was analyzed to form a baseline. Next, system models consisting entirely of the bridge rail and end terminals were simulated utilizing all three S3x5.7 (S76x8.5) posts models. All simulations were performed with the nominal impact severities prescribed for TL-3 of MASH. Prior full-scale crash testing of the MGS under test designation no. 3-11 produced a maximum deflection of 43.9 in. (1,114 mm) [3, 18], which demonstrated accuracy of the baseline model. For each post model, barrier deflections were found to be very similar to those observed in the MGS crash testing program, and pocketing angles were well below recommended limits. Results of these simulations are also summarized in Table 2. Thus, the simulation results demonstrated that a weak-post bridge rail system with reduced post spacing was capable of performing very similarly to the standard, strong-post MGS.

Following the simulations of the MGS and proposed bridge rail system, additional models were created to evaluate the need for an approach transition between the bridge rail design and the MGS. These models consisted of a 75-ft (22.86-m) long bridge rail positioned between two 50-ft (15.24-m) long guardrail systems. Numerous simulations were conducted, and it was determined that four criteria were used to evaluate the performance of the barrier system, including: (1) the largest pocketing angle in the approach interface; (2) the largest pocketing angle in the bridge rail system; (3) the largest pocketing angle in the departure interface; and (4) the largest lateral deflection in the overall barrier system. Post models for the guardrail and bridge rail were varied to create worst-case pocketing angles for each condition. For example, the worst-case pocketing angle in the approach guardrail (Case 1) was found from simulations performed on a barrier using the weaker guardrail post model and the strongest bridge rail post model. This configuration allowed for greater deflection in the guardrail along with a stiffer bridge rail response, thus generating higher pocketing angles.

All worst-case impact scenarios occurred in simulations with the 2270P vehicle. Maximum pocketing angles for all simulations were well below the recommended limit. The largest simulated pocketing angle of 25.9 degrees occurred in the approach interface when the barrier was simulated with the weaker guardrail post and the strongest bridge rail post models. A maximum system deflection of 52.4 in. (1,331 mm) occurred when the barrier was simulated with the weaker guardrail post and the weakest bridge rail post models. This larger deflection was aggravated by the small number of upstream guardrail posts, which placed a larger load on the upstream anchors and allowed more longitudinal rail displacement.

Following identification of the worst-case impact conditions, additional analyses were performed using the finer (449-node) mesh. In these simulations, the change in deflections between the coarser and finer meshes was very modest, indicating that the simulation findings had converged, further indicating good compatibility between the standard MGS and the bridge rail. Varying the properties of both the guardrail and bridge rail posts demonstrated that pocketing angles and deflections were well below recommended limits, even under worst-case scenarios. Further, comparison between BARRIER VII results and prior MGS full-scale tests indicated that the simulation results were accurate. Thus, preliminary simulations demonstrated that no special transition section was required at the interface between the MGS and the bridge rail. However, testing and calibration of the model was required to validate these results.

DESIGN DETAILS

A 175-ft (53.3-m) full-scale test installation was constructed with 68 ft - 9 in. (21.0 m) of bridge rail installed between two approach sections of MGS. Standard 12-gauge (2.66-mm thick) W-beam guardrail was used with a top mounting height of 31 in. (787 mm), and no transition sections were used at the guardrail-to-bridge rail interfaces. Photographs of the test installation are shown in Figure 1.

The bridge rail was constructed with ASTM A36 S3x5.7 (S76x8.5) posts spaced 37½ in. (953 mm) on center and placed in steel tubular deck attachment assemblies. These assemblies were anchored to the deck with a 1-in. (25.4-mm) diameter, SAE Grade 5 hex head bolt that passed through an upper steel strap which was welded to the tube and a lower steel angle which was bolted to the tube. Splices in the W-beam rail were located at bridge rail posts. No blockouts were used with the bridge rail, and 6-in. (152-mm) long, 12-gauge (2.66-mm thick) W-beam backup plates were used at all bridge rail post locations. The rail was connected to each post with a $^{5}/_{16}$-in. (7.9-mm) diameter, ASTM A307 Grade A bolt and nut along with a 1¾-in. x 1¾-in. x ⅛-in. (44-mm x 44-mm x 3-mm) ASTM A36 square washer.

An 8-in. (203-mm) thick, simulated reinforced concrete bridge deck was constructed for use in the crash testing and evaluation of the bridge rail. The specified minimum 28-day concrete compressive strength was 4,000 psi (27.6 MPa). All dowel bars and deck reinforcement were comprised of ASTM A615 steel. To aid with the installation of the bridge rail posts and minimize local deck damage, 2-in. x 2-in. x ¼-in. (51-mm x 51-mm x 6-mm) ASTM A500 Grade B square bolt-sleeves were cast into the deck. One no. 6 (19-mm diameter) rebar with a 5-in. (127-mm) diameter, 180-degree bend was looped around each bolt-sleeve near the deck surface using appropriate concrete cover. Additional bent no. 4 rebar was also placed above the upper reinforcement to the exterior of the bolt- sleeve assemblies, and longitudinal no. 6 bar was placed to the interior of each bolt-sleeve, just above the lower transverse reinforcement. Complete reinforcement details and test installation drawings are presented in the referenced reports [7, 8].

FULL SCALE CRASH TESTING

Longitudinal barriers, such as bridge rails, must satisfy the impact safety standards provided in MASH in order to be accepted by the Federal Highway Administration (FHWA) for use on National Highway System (NHS) new construction projects or as a replacement for existing designs not meeting current safety standards. According to TL-3 of MASH, longitudinal barrier systems must be subjected to two full-scale vehicle crash tests. The two full-scale crash tests are as follows:

1. Test Designation 3-10 consisting of a 2,425-lb (1,100-kg) passenger car impacting the system at a nominal speed and angle of 62 mph (100 km/h) and 25 degrees, respectively.
2. Test Designation 3-11 consisting of a 5,000-lb (2,268-kg) 4-door, half-ton pickup truck impacting the system at a nominal speed and angle of 62 mph (100 km/h) and 25 degrees, respectively.

The new bridge rail design described herein was evaluated using both of the required full-scale crash tests.

Full Scale Crash Test No. MGSBR-1

The 5,174-lb (2,347-kg) pickup truck, with a surrogate occupant placed in the left-front seat, impacted the bridge rail at a speed of 61.9 mph (99.6 km/h) and at an angle of 24.9 degrees. The point of impact was 15 ft - 9½ in. (4.81 m) upstream of the centerline of the splice at post no. 20. At 0.280 seconds, the vehicle became parallel to the system at a speed of 44.9 mph (72.3 km/h). The vehicle was contained and smoothly redirected and exited the system at 0.648 seconds at a speed of 34.5 mph (55.5 km/h) and at an angle of 20.4 degrees. All safety performance criteria were met. Thus, test no. MGSBR-1 was determined to be acceptable according to TL-3 of MASH. A summary of the test results and sequential photographs are shown in Figure 2, and test photographs are shown in Figure 3.

The maximum lateral dynamic rail deflection and working width of the system were 48.9 in. (1,242 mm) and 53.2 in. (1,351 mm), respectively. The length of vehicle contact along the system was approximately 34 ft - 3⅞ in. (10.5 m). Damage to the barrier was moderate, mainly consisting of deformed W-beam rail and bridge posts as well as splice extension due to membrane action of the rail. Additionally, one post mounting bracket was destroyed due to weld failure caused by wheel snag on the mounting bracket. The bridge deck sustained minor damage, including punching shear cracks on the outside edge of the deck at one post, lateral shear cracks at one location, and various amounts of spalling at ten posts. Note all cracks were narrow, no rebar was exposed, and the through-deck bolts and steel insert sleeves were not displaced. The damage to the vehicle was moderate, and all deformations were within acceptable limits as defined by MASH.

Full Scale Crash Test No. MGSBR-2

The 2,585-lb (1,173-kg) small car, with a surrogate occupant in the left-front seat, impacted the bridge rail at a speed of 62.3 mph (100.2 km/h) and at an angle of 24.9 degrees. The point of impact was 7 ft - 9 in. (2.36 m) upstream of the centerline of the splice at post no. 20. At 0.298 seconds, the vehicle became parallel to the system at a speed of 31.2 mph (50.3 km/h). The vehicle was contained and smoothly redirected exited the system at 0.582 seconds at a speed of 27.7 mph (44.6 km/h) and at an angle of 10.9 degrees. All safety performance criteria were met. Thus, test no. MGSBR-2 was determined to be acceptable according to TL-3 of MASH. A summary of the test results and sequential photographs are shown in Figure 4, and test photographs are shown in Figure 5.

The maximum lateral dynamic rail deflection and working width of the system were 28.0 in. (712 mm) at post no. 21 and 33.8 in. (859 mm), respectively. The length of vehicle contact along the system was approximately 22 ft - 8 in. (6.91 m). Damage to the barrier was moderate, mainly consisting of deformed W-beam rail and bridge posts as well as splice extension due to membrane action of the rail. Minor damage was sustained by the mounting brackets, consisting of slightly bent backside retainer plates and lower bracket connection bolts. The bridge deck sustained minor damage, including deck cracking at five posts and spalling at several posts. Severe cracking occurred at one post; however, the through-deck bolt and bolt sleeve were not displaced. The damage to the vehicle was moderate, and all deformations to the vehicle were well below recommended limits presented in MASH.

TRANSITION EVALUATION

BARRIER VII Model Calibration

Following the full-scale crash tests, additional BARRIER VII simulations were conducted to calibrate the barrier model with the full-scale test results and further evaluate the transition between the MGS system and the bridge rail. BARRIER VII models for the bridge rail posts and the coefficient of friction between the vehicle and the bridge rail were calibrated to match the test results. Recall that three different S3x5.7 post models were used in the pre-test modeling. Simulations of both full-scale tests demonstrated that the weakest of the three post models provided the most accurate results. In addition, while BARRIER VII does not include the effects of wheel snag in its analysis, the effect of this phenomenon on vehicle trajectory can be simulated by adjusting the coefficient of friction. Since the pickup and small car have different snag characteristics, separate friction coefficients were required for each test. Three different contact interfaces were specified in the updated BARRIER VII models. Two contact interfaces were defined for the approach guardrails using the previous coefficient of friction of 0.35, and one contact interface was defined for the bridge rail.

2270P Test Calibration

The simulation model of test no. MGSBR-1 was calibrated with a coefficient of friction of 0.23. This value was considerably lower than that of the original MGS BARRIER VII model, but it was thought to be sufficiently accurate due to the different nature of the snag. Many of the bridge rail posts snagged on the pickup truck near the center of its front bumper, whereas snag occurs closer to the edge of a vehicle due in the MGS. This difference was caused by several factors. First, the approach guardrail uses blockouts, whereas the bridge rail does not. Additionally, while the center of rotation of guardrail posts is beneath the ground surface, the bridge rail posts bend at the top of the bridge deck. Deflections in both systems are similar, thus the vehicle overrode posts to a greater extent in the bridge rail. This allows for snag to occur near the vehicle's center, which does not apply a moment to resist vehicle redirection, whereas in the guardrail, post snag does resist redirection. Thus, a lower coefficient of friction was used for the bridge rail. A comparison of simulation and physical test results for test no. MGSBR-1 is shown in Table 3. Dynamic deflection was predicted to within 10% of the physical test value, while predicted parallel time, length of contact, and permanent set deflections were nearly identical to those observed in the full-scale test.

Graphical comparisons of the simulated and physical barrier deflections showed that the model predicted a reasonably accurate deflected shape of the barrier. Deflections were slightly underestimated around the point of vehicle contact, and slightly overestimated upstream and downstream of vehicle contact.

The model showed significant error in predicting vehicle speeds due to limitations of the BARRIER VII analysis. In the full-scale test, the pickup truck overrode approximately nine posts as it protruded beyond the edge of the deck. Therefore, the vehicle was decelerated without affecting redirection due to the center of the vehicle contacting posts, which could not be simulated using the coefficient of friction. The left-front wheel of the vehicle also detached from the vehicle, and the vehicle had to be pulled back onto the deck by the barrier after protruding beyond the edge. Both of these events dissipated significant amounts of energy and could not be

simulated, thus inhibiting the ability of BARRIER VII to accurately predict the pickup truck's velocity.

Error was also present in the simulated number of failed posts. BARRIER VII deleted post elements when the rail deflected more than 15 in. (381 mm). Rail deflection exceeded this value at only nine posts, nos. 16 through 24, in the physical test, whereas BARRIER VII predicted eleven failed posts, nos. 15 through 25. However, in the physical test, post no. 15 deflected 14.9 in. (378 mm) which demonstrates better agreement between the simulation and the test. As discussed previously, the exit velocity of the simulated truck was greater than that observed for the physical truck due to the energy-absorbing mechanisms that could not be simulated. As a result the simulated pickup truck deflected the downstream guardrail to a greater extent, with a greater number of failed posts.

1100C Test Calibration

The simulation model of test no. MGSBR-2 was calibrated with a coefficient of friction of 0.525. The coefficient of friction was much higher for the small car than for the pickup due to increased vehicle snag on the closely spaced, non-blocked bridge rail posts. Barrier deflection was less in the small car test, causing post snag to occur near the edge of the vehicle and resist redirection. The rail also deformed the left-front corner of the car inward to a greater extent than observed for the pickup truck, creating increased interlock between the vehicle and the rail.

A comparison of simulation and physical test results for test no. MGSBR-2 is shown in Table 4. Note that predicted dynamic deflection, permanent set deflection, and parallel time were nearly identical to the values from the full-scale test. Graphical comparisons of the simulated and physical barrier deflections showed that the simulation predicted excellent results for the deformed shape of the barrier.

Eight posts failed during full-scale testing, whereas BARRIER VII predicted only 4 post failures. Many of the physical posts failed due to wheel snag, whereas BARRIER VII only considered post failure to occur when the rail deflection exceeded 15 in. (381 mm) at a post location. Dynamic deflection data for the rail, obtained from high-speed video analysis, demonstrated that the rail deflected more than 15 in. (381 mm) at five post locations. Thus, the BARRIER VII prediction of four of failed posts matches the full-scale test results much more closely when compared with this criterion.

While length of contact differed between the simulation and the physical crash test, the deflected shape of the rail matched very well. Contact observed in the physical test was due to the vehicle overhang off the bridge deck, which caused the car to roll toward and contact the rail even after it was redirected, which could not be simulated in BARRIER VII.

Bridge Rail-to-Guardrail Interface Analysis

Transition sections are required when a more flexible barrier connects to a less flexible barrier and allows a vehicle to pocket behind the stiffer barrier, consequently generating dangerous accelerations and/or vehicle instabilities. As the bridge rail proved to be more flexible than the standard MGS, the potential for vehicle pocketing existed for impacts originating on the bridge rail and continuing into the guardrail. However, the relative flexibility of the bridge rail ensured that impacts which originated in the approach guardrail and continued into the bridge rail would not experience unacceptable pocketing angles. Thus, only the bridge rail-to-guardrail interface required additional investigation.

Pocketing angles were only a concern for the pickup truck, since the small car did not deflect the system sufficiently to become pocketed. Thus, additional analyses were only performed with the pickup truck model. While the calibrated barrier model for test no. MGSBR-1 produced good results, it underestimated deflection by approximately 10%. Vehicle deflections into the upstream barrier were considered critical to accurately evaluate pocketing in the downstream barrier. Underestimating deflection could lead to an underestimation of pocketing angles and produce unacceptable results. To eliminate this problem, the bridge rail post models were weakened such that the simulated deflection matched the measured deflection. The yield moment of the bridge rail posts was reduced from 82 kip-in. (9.26 kN-m) to 74.5 kip-in. (8.42 kN-m).

Thirty-three simulations were performed with the 225-node model for points of impact spanning from six post spaces upstream from the downstream end of the bridge rail through the first guardrail post. These impacts were spaced 9⅜ in. (238 mm) along the bridge rail. The simulation predicting the largest pocketing angle was conducted utilizing the 449-node model to ensure that mesh density did not adversely affect the analysis results.

The effects of snag were not considered in the analysis for several reasons. First, the MGS has been previously tested with high flare rates [22], during which the pickup truck deflected the system over 75 in. (1,905 mm). Such deflections ensure interaction between the vehicle's wheels and the posts. In these tests, snag was not found to be problematic. The left-front wheel of the pickup truck also detached during test no. MGSBR-1. Similar behavior was expected for impacts throughout the bridge rail, and detachment of this wheel from the pickup truck would make wheel snag on a guardrail post nearly impossible.

BARRIER VII simulations demonstrated that pocketing angles of pickup truck impacts in the bridge rail-to-guardrail interface were well below recommended limits. The largest pocketing angles occurred when the vehicle impacted at the midspan between the last bridge rail post and the first guardrail post. This produced maximum 3-node and 5-node pocketing angles of 19.6 degrees and 19.5 degrees, respectively. When simulated with the finer mesh, this impact event produced maximum 3-node and 5-node pocketing angles of 19.1 degrees and 18.4 degrees, respectively.

The impact condition that produced maximum pocketing was essentially an impact on the guardrail itself. Thus, pocketing angles for impacts in the downstream MGS are greater than for impacts in the transition section. All impacts which began upstream of the last bridge rail posts generated maximum 3-node and 5-node pocketing angles of less than 18.2 degrees and 17.5 degrees, respectively, which were well below recommended values. Therefore, the bridge rail was believed to perform adequately with a direct attachment to the MGS, and a transition section was not needed.

SUMMARY AND CONCLUSIONS

A new, weak-post bridge rail was developed that satisfies the TL-3 safety performance criteria presented in MASH. This new bridge rail has a lateral stiffness and strength comparable to that of the MGS. Therefore, the bridge rail system may be directly connected to the MGS without the use of an approach guardrail transition section. As such, the additional post and rail elements typically required by transition sections have been eliminated, and barrier cost and complexity are reduced. Since the new bridge rail utilizes posts mounted on the side of the deck and does not require blockouts, encroachment of the bridge rail onto the bridge deck is minimized. Repair of the new bridge rail is simple and should typically only require replacement of steel posts, W-

beam rail, and post-to-rail connection hardware. Further, the new bridge rail will provide a safer alternative to many existing bridge railings now in use on local roads and streets across the nation.

Deck damage was deemed acceptable and can be further mitigated through the implementation of design revisions. Both lateral and vertical shear cracking can be reduced through the use of higher strength concrete and a thicker bridge deck. Lateral shear cracking can be further mitigated by locating the through-deck bolt and bolt sleeve farther inward on the deck or by designing the deck reinforcement to more quickly develop resistive forces. This modification could be accomplished by using two smaller diameter bars and a smaller bend diameter for the reinforcing loop or welding the bars to the bolt sleeve. Vertical shear cracks could be further mitigated by using a wider and thicker top mounting plate, using larger upper and lower longitudinal bars at the exterior edge of the bridge deck, or using U-shaped transverse reinforcement.

Spalling may be reduced by eliminating the ½-in. (13-mm) gap between the deck edge and the mounting bracket. This change would reduce the downward prying action of the assembly and the downward deflection of the top mounting plate, thus decreasing the propensity for the mounting tube to impact the top corner of the deck. Alternatively, a bearing pad could be placed in the gap. Finally, chamfering the outer edges of the deck may also reduce spalling.

One mounting bracket was destroyed during the first full-scale test. This failure may be avoided by increasing the weld size, adding a second gusset plate, thickening the top mounting plate, and/or extending the top mounting plate around both sides of the mounting tube. Alternatively, the mounting tube could be cast into the deck.

Although W-beam backup plates were used in the bridge rail, they may not be necessary. Inspection of high-speed video as well as the post-test installation hardware revealed that post contact marks on the rail were beyond the reach of the backup plates, and that the sharp edges of the post flanges did not contact the rail. Thus, W-beam backup plates may not be warranted. However, this and all recommended design revisions may require additional analysis or crash testing before they can be safely implemented.

The new bridge rail should provide a low-cost alternative to traditional bridge rails. When compared with an open concrete rail, the new bridge rail is estimated to cost between $8,000 and $13,000 less to install on a 75-ft long bridge [7].

For the bridge rail to be safely used on alternate bridge decks, users must ensure the deck has adequate structural capacity to resist the imparted rail loads. The simulated bridge deck was designed for a peak post force of 6.3 kips (28.0 kN) at the center-height of the rail. The bolt sleeve was also designed to resist bending and prevent local damage to the top of the concrete deck. Designers should also be aware of other significant loads that are imparted into the deck, including downward loads due to prying action of the mounting brackets and vehicle override of bridge rail posts, and additional lateral shear loads caused by vehicle snag on posts. Though these loads cannot be accurately quantified at this time, designers should be aware of these forces and design accordingly.

Full-scale testing was performed on a bridge deck without a wearing surface. Should such a wearing surface be placed above the top mounting plate, post and mounting tube length should be modified accordingly to ensure similar resistive forces are developed by the posts. The top mounting plate of the new bridge rail extends beyond the front face of the W-beam rail. Thus, the plate and through-deck bolt would be susceptible to damage from snow-plow operations on bridge decks without a wearing surface. This potential concern could be eliminated by using a 4-

in. (102-mm) deep blockout between the W-beam rail and steel posts. However, additional analysis or testing is required before alternate rail mounting details can be recommended.

DISCLAIMER

The contents of this report reflect the views of the authors who are responsible for the facts and the accuracy of the data presented herein. The contents do not necessarily reflect the official views or policies of the Federal Highway Administration nor the state highway departments participating in the Midwest States Regional Pooled Fund Program. This report does not constitute a standard, specification, or regulation.

ACKNOWLEDGEMENTS

The authors wish to acknowledge several sources that made a contribution to this project: (1) the Midwest States Regional Pooled Fund Program for sponsoring the research project and (2) MwRSF personnel for constructing the barriers and conducting the crash tests.

REFERENCES

1. *Manual for Assessing Safety Hardware (MASH)*, American Association of State and Highway Transportation Officials, Washington, D.C., 2009.

2. Polivka, K.A, Faller, R.K., Sicking, D.L., Reid, J.D., Rohde, J.R., Holloway, J.C., Bielenberg, R.W., and Kuipers, B.D., *Development of the Midwest Guardrail System (MGS) for Standard and Reduced Post Spacing and in Combination with Curbs*, Final Report to the Midwest States Regional Pooled Fund Program, Transportation Research Report No. TRP-03-139-04, Midwest Roadside Safety Facility, University of Nebraska-Lincoln, September 1, 2004.

3. Polivka, K.A., Faller, R.K., Sicking, D.L., Rohde, J.R., Bielenberg, B.W., and Reid, J.D., *Performance Evaluation of the Midwest Guardrail System - Update to NCHRP 350 Test No. 3-11 with 28" C.G. Height (2214MG-2)*, Final Report to the National Cooperative Highway Research Program (NCHRP), Transportation Research Board, Transportation Research Report No. TRP-03-171-06, Midwest Roadside Safety Facility, University of Nebraska-Lincoln, October 11, 2006.

4. Polivka, K.A., Faller, R.K., Sicking, D.L., Rohde, J.R., Bielenberg, B.W., and Reid, J.D., *Performance Evaluation of the Midwest Guardrail System - Update to NCHRP 350 Test No. 3-10 (2214MG-3)*, Final Report to the National Cooperative Highway Research Program (NCHRP), Transportation Research Board, Transportation Research Report No. TRP-03-172-06, Midwest Roadside Safety Facility, University of Nebraska-Lincoln, October 11, 2006.

5. Sicking, D.L., Reid, J.D., and Rohde, J.R., *Development of the Midwest Guardrail System*, Transportation Research Record 1797, TRB, National Research Council, Washington, D.C., November 2002, pp. 44-52.

6. Faller, R.K., Polivka, K.A., Kuipers, B.D., Bielenberg, B.W., Reid, J.D., Rohde, J.R., and Sicking, D.L., *Midwest Guardrail System for Standard and Special Applications*, Transportation Research Record No. 1890, Journal of the Transportation Research Board, TRB AFB20 Committee on Roadside Safety Design, Transportation Research Board, Washington, D.C., January 2004.

7. Thiele, J.C., Development of a Low-Cost, Energy-Absorbing Bridge Rail, Thesis, University of Nebraska-Lincoln, December 2009.

8. Thiele, J.C., Sicking, D.L., Faller, R.K., Bielenberg, R.W., Lechtenberg, K.A., Reid, J.D., and Rosenbaugh, S.K., *Development of a Low-Cost, Energy-Absorbing, Bridge Rail*, Draft Report to the Midwest States Regional Pooled Fund Program, Transportation Research Report No. TRP-03-226-10, Midwest Roadside Safety Facility, University of Nebraska-Lincoln, 2010.

9. Mak, K.K., Bligh, R.P., and Menges, W.L., *Testing of State Roadside Safety Systems Volume XI: Appendix J – Crash Testing and Evaluation of Existing Guardrail Systems*, Report No. FHWA-RD-95, Texas Transportation Institute, Texas A&M University, College Station, Texas, December 1995.

10. Engstrand, K.E., Improvements to the Weak-Post W-Beam Guardrail, Thesis, Worcester Polytechnic Institute, Worcester, Massachusetts, June 2000.

11. Ray, M.H., Engstrand, K., Plaxico, C.A., and McGinnis, R.G., *Improvements to the Weak-Post W-Beam Guardrail,* Transportation Research Record 1743, Transportation Research Board, Washington, D.C., 2001.

12. Kilareski, W.P., El-Gindy, M., St. John, B.D., and Pecheux, B., *Type 2 Weak Post Guiderail Testing*, Submitted to Pennsylvania Department of Transportation, Report No. PTI 9925, Agreement No. 359704, Work Order 20, Pennsylvania Transportation Institute, Penn State University, University Park, Pennsylvania, February 1999.

13. Buth, C.E., Menges, W.L., and Schoeneman, S.K., *NCHRP Report 350 Test 3-11 on the Modified PennDOT Type 2 Guide Rail,* Project No. RF473750-1, Texas Transportation Institute, Texas A&M University, College Station, Texas, January 2000.

14. Powell, G.H., *Barrier VII: A Computer Program for Evaluation of Automobile Barrier Systems,* Report No. FHWA-RD-73-51, Department of Civil Engineering, University of California, Berkeley, California, April 1973.

15. Eller, C.M., Polivka, K.A., Faller, R.K., Sicking, D.L., Rohde, J.R., Reid, J.D., Bielenberg, R.W., and Allison, E.M., *Development of the Midwest Guardrail System (MGS) W-Beam to Thrie Beam Transition Element*, Final Report to the Midwest States Regional Pooled Fund Program, MwRSF Research Report No. TRP-03-167-07, Midwest Roadside Safety Facility, University of Nebraska-Lincoln, November 26, 2007.

16. Rosenbaugh, S.K., Lechtenberg, K.A., Faller, R.K., Sicking, D.L., Reid, J.D., and Bielenberg, R.W., *Development of the MGS Approach Guardrail Transition Using Steel*

and Wood Standardized Posts, Draft Report to the Midwest States Regional Pooled Fund Program, MwRSF Research Report No. TRP-03-210-10, Midwest Roadside Safety Facility, University of Nebraska-Lincoln, 2010.

17. Kuipers, B.D. and Reid, J.D., *Testing of M203x9.7 (M8x6.5) and S76x8.5 (S3x5.7) Steel Posts – Post Comparison Study for the Cable Median Barrier,* Final Report to the Midwest States Regional Pooled Fund Program, MwRSF Report No. TRP-03-143-03, Midwest Roadside Safety Facility, University of Nebraska-Lincoln, October 2003.

18. Faller, R.K., Sicking, D.L., Bielenberg, R.W., Rohde, J.R., Polivka, K.A., and Reid, J.D., *Performance of Steel-Post, W-Beam Guardrail Systems*, Transportation Research Record 2025, TRB, National Research Council, Washington, D.C., January 2008, pp. 18-33.

19. Kuipers, B.D., and Reid, J.D., *Testing of W152x23.8 (W6x16) Steel Posts – Soil Embedment Depth Study for the Midwest Guardrail System*, Final Report to the Midwest States Regional Pooled Fund Program, MwRSF Research Report No. TRP-03-136-03, Midwest Roadside Safety Facility, University of Nebraska-Lincoln, June 12, 2003.

20. Kuipers, B.D., Faller, R.K., and Reid, J.D., *Critical Flare Rates for W-Beam Guardrail – Determining Maximum Capacity Using Computer Simulation*, Final Report to the Midwest States Regional Pooled Fund Program, MwRSF Research Report No. TRP-03-136-03, Midwest Roadside Safety Facility, University of Nebraska-Lincoln, January 24, 2005.

21. *AASHTO LRFD Bridge Design Specifications, 4th Edition*, American Association of State Highway and Transportation Officials, Washington, D.C., 2007.

22. Stolle, C.S., Polivka, K.A., Reid, J.D., Faller, R.K., Sicking, D.L., Bielenberg, R.W., and Rohde, J.R., *Evaluation of Critical Flare Rates for the Midwest Guardrail System (MGS)*, Final Report to the Midwest States Regional Pooled Fund Program, MwRSF Report No. TRP-03-191-08, Midwest Roadside Safety Facility, University of Nebraska-Lincoln, July 15, 2008.

LIST OF TABLES AND FIGURES

Table 1. Static Testing Results

Concept	Bolt Diameter	Location of Bolt in Slot	No. of Guardrail Layers	Peak Force	Failure Type
G2 Post-to-Rail Connection	$^{5}/_{16}$ in. (7.9 mm)	Edge	2	4.3 kips (18.7 kN)	Bolt Fracture
G2 Post-to-Rail Connection	$^{5}/_{16}$ in. (7.9 mm)	Center	1	2.8 kips (12.6 kN)	Washer Pull-Through
G2 Post-to-Rail Connection	⅜ in. (9.5 mm)	Edge	2	5.8 kips (25.7 kN)	Bolt Pull-Through

Table 2. Guardrail-Only and Bridge Rail-Only Results (225-Node)

System	Post Model	Vehicle	Maximum Barrier Deflection		Maximum 5-Node Pocketing	
			Deflection in. (mm)	Distance from Impact – ft (m)	Angle (deg)	Distance from Impact – ft (m)
MGS	W6x8.5	2270P	43.4 (1,102)	15.6 (4.8)	16.0	10.9 (3.3)
Bridge Rail	S3x5.7 90-deg	2270P	40.1 (1,019)	14.1 (4.3)	21.2	19.5 (5.9)
Bridge Rail	S3x5.7 75-deg	2270P	43.5 (1,105)	15.6 (4.8)	19.4	21.1 (6.4)
Bridge Rail	S3x5.7 60-deg	2270P	46.3 (1,175)	16.4 (5.0)	17.7	21.9 (6.7)
MGS	W6x8.5	1100C	26.7 (678)	8.6 (2.6)	14.3	9.4 (2.9)
Bridge Rail	S3x5.7 90-deg	1100C	23.7 (602)	7.8 (2.4)	15.9	10.2 (3.1)

Figure 1. System Details

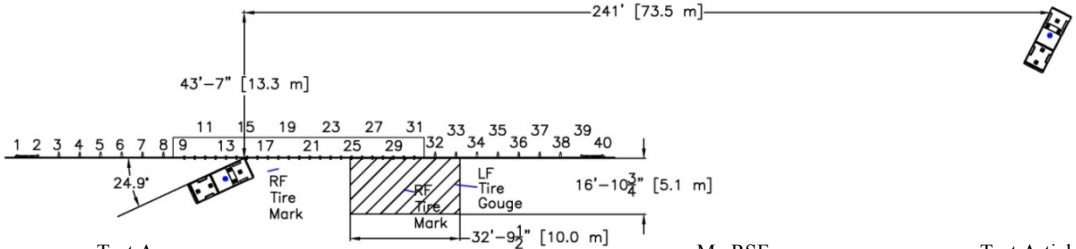

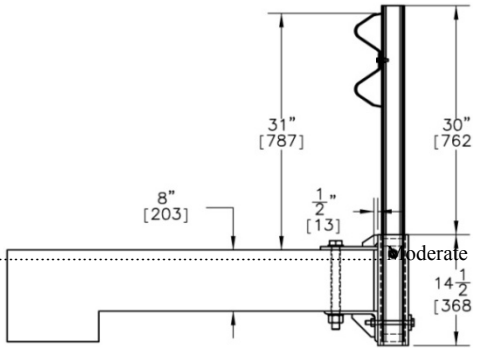

- Test Agency ..... MwRSF
- Test Number MGSBR-1
- Date 6/18/2009
- MASH Test Designation 3-11
- Test Article ..... MGS Bridge Rail with approach MGS Guardrails
- Total Length ..... 175 ft (53.3 m)
- Key Component – MGS Bridge Rail
  - Post Type S3x5.7 (S76x8.5)
  - Post Spacing ..... 3 ft - 1½ in. (953 mm)
  - Post-to-rail Connection ..... $\frac{5}{16}$-in. (7.9-mm) dia. ASTM A307A Grade A Bolt
  - Mounting Bracket ..... 4x4x⅜ (102x102) ASTM A572 Tube
  - Deck Connection ..... 1-in. (25.4-mm) dia. Grade 5 Bolt
- Key Component – Simulated Bridge Deck
  - Thickness (outer edge) ..... 8 in. (203 mm)
  - Minimum 28-day Concrete Strength ..... 4,000 psi (27.6 MPa)
- Vehicle Model ..... 2004 Dodge Ram 1500 Quad Cab Pickup Truck
  - Curb ..... 5,134 lb (2,329 kg)
  - Test Inertial ..... 5,005 lb (2,270 kg)
  - Gross Static ..... 5,174 lb (2,347 kg)
- Impact Conditions
  - Speed ..... 61.9 mph (99.6 km/h)
  - Angle ..... 24.9 degrees
  - Impact Location ..... 15 ft - 9½ in. (4.81 m) US of post no. 20 splice
- Exit Conditions
  - Speed ..... 34.5 mph (55.5 km/h)
  - Angle ..... 20.4 degrees
  - Exit Box ..... Pass
- Vehicle Stability ..... Satisfactory
- Vehicle Stopping Distance ..... 241 ft (73.5 m) downstream
  43 ft - 7 in. (13.3 m) behind edge of bridge deck
- Vehicle Damage ..... Moderate
  - VDS 11-LFQ-3
  - CDC 11-LYEW-4
  - Maximum Interior Deformation ..... 1¾ in. (44 mm), left side panel
- Test Article Damage ..... Moderate
- Test Article Deflections
  - Permanent Set ..... 31⅞ in. (810 mm)
  - Dynamic ..... 48.9 in. (1,242 mm)
  - Working Width ..... 53.2 in. (1,351 mm)
- Angular Displacements (EDR-4)
  - Roll ..... -15.3 degrees
  - Pitch ..... -5.6 degrees
  - Yaw ..... 37.8 degrees
- Angular Displacements (DTS)
  - Roll ..... -14.0 degrees
  - Pitch ..... -5.4 degrees
  - Yaw ..... 39.8 degrees

Transducer Data					
Evaluation Criteria		Transducer			MASH Limit
		EDR-4	DTS	EDR-3	
OIV ft/s (m/s)	Longitudinal	-16.94 (-5.16)	-16.86 (-5.14)	-18.84 (-5.74)	≤ 40 (12.2)
	Lateral	13.27 (4.04)	14.23 (4.34)	14.18 (4.32)	≤ 40 (12.2)
ORA g's	Longitudinal	-10.61	-10.44	-12.55	≤ 20.49
	Lateral	5.42	6.33	5.61	≤ 20.49
THIV – ft/s (m/s)		20.66 (6.30)	21.03 (6.41)	N/A	not required
PHD – g's		10.64	10.50	N/A	not required
ASI		0.53	0.57	0.64	not required

Figure 2. Summary of Test Results and Photographs, Test No. MGSBR-1

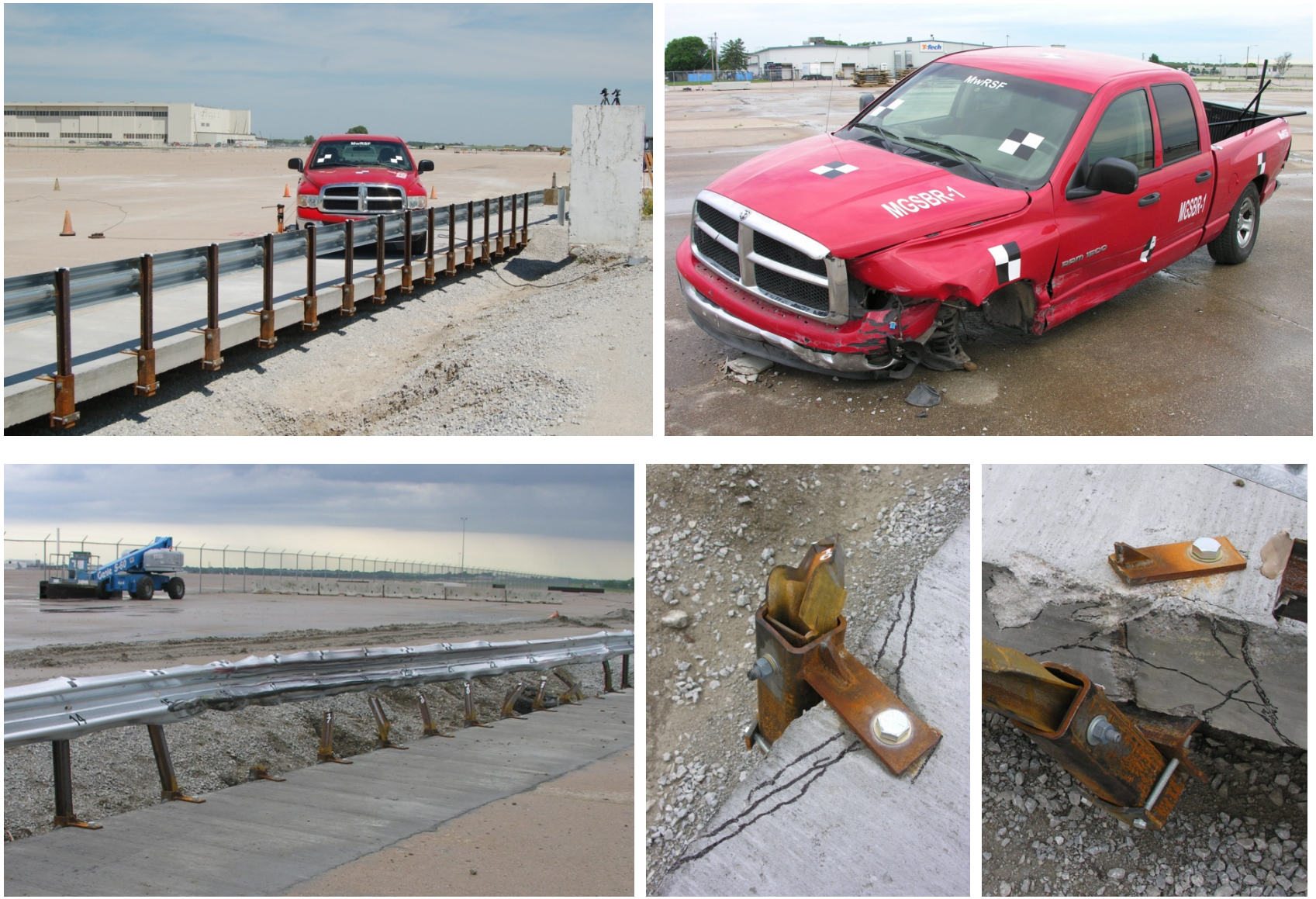

Figure 3. Impact Location, Vehicle Damage, and System Damage, Test No. MGSBR-1

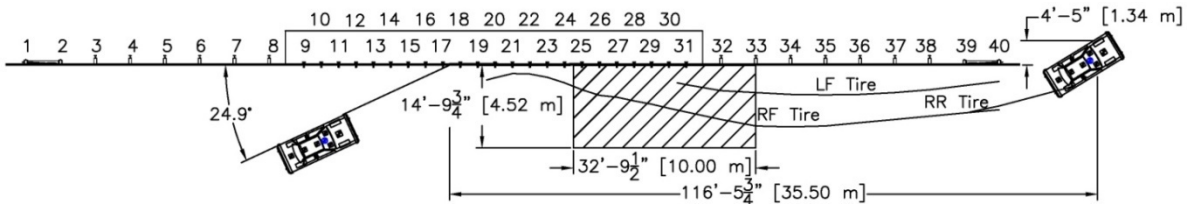

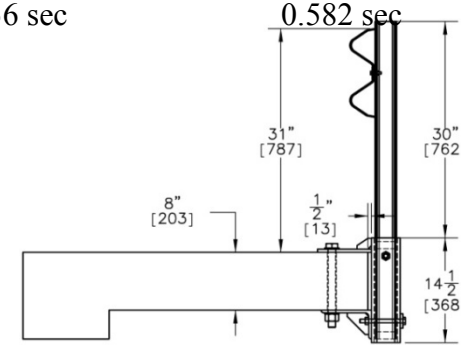

- Test Agency ..... MwRSF
- Test Number MGSBR-2
- Date 6/26/2009
- MASH Test Designation 3-10
- Test Article ..... MGS Bridge Rail with approach MGS Guardrails
- Total Length ..... 175 ft (53.3 m)
- Key Component – MGS Bridge Rail
  - Post Type S3x5.7 (S76x8.5)
  - Post Spacing ..... 3 ft - 1½ in. (953 mm)
  - Post-to-rail Connection ..... 5/16-in. (7.9-mm) dia. ASTM A307A Bolt
  - Mounting Bracket ..... 4x4x⅜ (102x102x102) ASTM A572 Tube
  - Deck Connection ..... 1-in. (25.4-mm) dia. Grade 5 Bolt
- Key Component – Simulated Bridge Deck
  - Thickness (outer edge) ..... 8 in. (203 mm)
  - Minimum 28-day Concrete Strength ..... 4,000 psi (27.6 MPa)
- Vehicle Model ..... 2003 Kia Rio Passenger Car
  - Curb ..... 2,408 lb (1,092 kg)
  - Test Inertial ..... 2,416 lb (1,096 kg)
  - Gross Static ..... 2,585 lb (1,173 kg)
- Impact Conditions
  - Speed ..... 62.3 mph (100.2 km/h)
  - Angle ..... 24.9 degrees
  - Impact Location ..... 7 ft - 9 in. (2.36 m) US of the splice at post no. 20
- Exit Conditions
  - Speed ..... 27.7 mph (44.6 km/h)
  - Angle ..... 10.9 degrees
  - Exit Box ..... Pass
- Vehicle Stability ..... Satisfactory
- Vehicle Stopping Distance ..... 116 ft - 5¾ in. (35.5 m) downstream
  4 ft - 5 in. (1.3 m) behind front face of guardrail
- Vehicle Damage ..... Moderate
  - VDS 11-LFQ-4
  - CDC 11-LYEW-5
  - Maximum Interior Deformation ..... 1¼ in. (32 mm), front of floor pan
- Test Article Damage ..... Moderate
- Test Article Deflections
  - Permanent Set ..... 20 in. (508 mm)
  - Dynamic ..... 28.0 in. (712 mm)
  - Working Width ..... 33.8 in. (859 mm)
- Angular Displacements (EDR-4)
  - Roll ..... -8.7 degrees
  - Pitch ..... -8.2 degrees
  - Yaw ..... 34.7 degrees
- Angular Displacements (DTS)
  - Roll ..... -12.7 degrees
  - Pitch ..... -5.0 degrees
  - Yaw ..... 35.1 degrees
- Transducer Data

Evaluation Criteria		Transducer			MASH Limit
		EDR-4	DTS	EDR-3	
OIV ft/s (m/s)	Longitudinal	-24.40 (-7.44)	-22.90 (-6.98)	-25.29 (-7.71)	≤ 40 (12.2)
	Lateral	16.54 (5.04)	16.38 (4.99)	17.94 (5.47)	≤ 40 (12.2)
ORA g's	Longitudinal	-7.69	-7.41	-8.65	≤ 20.49
	Lateral	6.58	7.34	7.39	≤ 20.49
THIV – ft/s (m/s)		28.50 (8.69)	28.04 (8.55)	N/A	not required
PHD – g's		9.93	9.90	N/A	not required
ASI		0.79	0.78	0.88	not required

Figure 4. Summary of Test Results and Photographs, Test No. MGSBR-2

Figure 5. Impact Location, Vehicle Damage, and System Damage, Test No. MGSBR-2

Table 3. Calibrated BARRIER VII Simulation Results, Test No. MGSBR-1

Evaluation Criteria	Physical Test Results	BARRIER VII Results	Error
Dynamic Deflection - in. (mm)	48.9 (1,242)	44.0 (1,118)	-10.0%
Permanent Set Deflections - in. (mm)	31.9 (810)	32.2 (818)	0.9%
Length of Contact - in. (mm)	411.9 (10,462)	409.3 (10,396)	-0.6%
Failed Posts (>15 in. rail deflection)	16-24	15-25	2 posts
Parallel Time - msec	280	281	0.4%
Parallel Speed - mph (km/h)	44.9 (72.3)	47.7 (76.8)	6.2%
Exit Time - msec	648	544	-16.0%
Exit Speed - mph (km/h)	34.5 (55.5)	44.4 (71.5)	28.7%

Table 4. Calibrated BARRIER VII Simulation Results, Test No. MGSBR-2

Evaluation Criteria	Physical Test Results	BARRIER VII Results	Error
Dynamic Deflection - in. (mm)	28.0 (711)	27.9 (709)	-0.4%
Permanent Set Deflections - in. (mm)	20.0 (508)	21.0 (533)	5.0%
Length of Contact - in. (mm)	272.0 (6,909)	203.4 (5,166)	-25.2%
Failed Posts (>15 in. rail deflection)	18-22	19-22	1 post
Parallel Time - msec	298	298	0.0%
Parallel Speed - mph (km/h)	31.2 (50.3)	31.9 (51.3)	2.2%
Exit Time - msec	582	493	-15.3%
Exit Speed - mph (km/h)	27.7 (44.6)	30.4 (48.9)	9.7%